

Autonomous Cam-Follower Transformable Wheel Robot

Siyuan Li¹, Juntao Wu², Sergio Aman Soetomo³, Hock Jin Koh⁴

Abstract— This paper presents the design and manufacturing of an autonomous vehicle that is capable of maneuvering through multiple terrains. The key factor to having such maneuverability is transformable wheels. Transformable wheels have become critical in the improvement of the performances of vehicles due to their superior traction, stability, and shock absorption compared to rigid wheels. As a result, we developed transformable wheels, with references to current research, to create an autonomous vehicle which was able to maneuver through rough and sandy surfaces. The developed transformable wheel utilizes a cam-follower-spring structure, which is simple to manufacture, low in cost, and highly efficient in terms of space utilization. The design and manufacturing process of the hardware, as well as the design of the control system used in the software, is described in detail in this paper. Overall, our autonomous transformable wheel vehicle has demonstrated that it can navigate through various test terrains, pass through height restrictions, traverse sand, and climb stairs.

I. INTRODUCTION

In recent years, the navigation technology and autonomous driving algorithms for robots have become increasingly sophisticated [10]. However, most of these robot structures and algorithms are designed for well-maintained road surfaces [8]. Research on robots capable of navigating diverse terrains and harsh environments is relatively scarce [10]. Nonetheless, this research is crucial as such robots can be used in post-disaster rescue operations and the exploration of unknown terrains [8]. A crucial element in achieving this level of maneuverability lies in the design and implementation of transformable wheels. We aim to develop an autonomous exploration robot equipped with easily manufacturable transformable wheels.

The primary objective of this research is to design and manufacture an autonomous vehicle equipped with transformable wheels capable of seamlessly traversing multiple terrains, including climbing up steps, going through terrain with height limiting and sandy surfaces. Our main advancement is the innovative transformable wheel and that the car can automatically determine its deployment state and steering requirements based on the current terrain, thereby reducing the need for manual intervention. Our transformable wheel utilizes a cam-follower-spring structure, which is simple to manufacture, low in cost, and highly efficient in terms of space utilization. This paper details the comprehensive process of developing these wheels, from initial conceptualization to final manufacturing, incorporating insights from current research and advancements in wheel technology.

In addition to the hardware development, this paper also delves into the design of the control system that governs

the vehicle's operation. We used a Raspberry Pi as the main control board, along with ultrasonic sensors and a camera to determine the car's current position and terrain environment. We developed corresponding algorithms that allow the car to automatically expand or retract based on the current terrain. Additionally, we employed a PID algorithm to enable obstacle avoidance and ensure straight-line movement.

The literature review of various autonomous vehicles is shown in *Appendix 1*.

II. DESIGN - SYNTHESIS

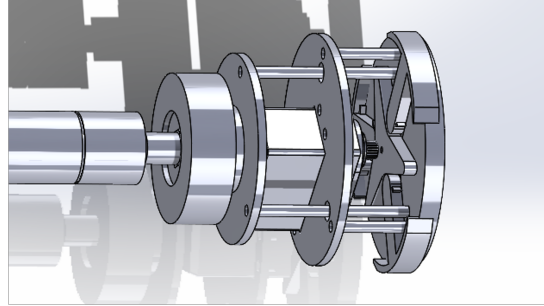


Fig. 1: Design of the Transformable Wheel

Towards the end of the development of our autonomous vehicle, our vehicle must be able to maneuver through different surfaces, climb through obstacles, as well as be able to self-park using transformable wheels with springs, geared motors, cam and followers, servo motors, ultrasonic sensors, and a camera. The detailed results of our development in autonomous vehicles and transformable wheels can be found in the next section of the report.

A. Two Wheel Design

The movement of the vehicle is powered by geared DC motors. Each wheel has a DC motor that drives the wheel through the use of a slip ring. The slip ring ensures the wires do not curl up when the vehicle is moving. Within each wheel, a servo motor is attached to control the extension and retraction of the claws on the wheel.

*The authors are all from UM-SJTU Joint Institute

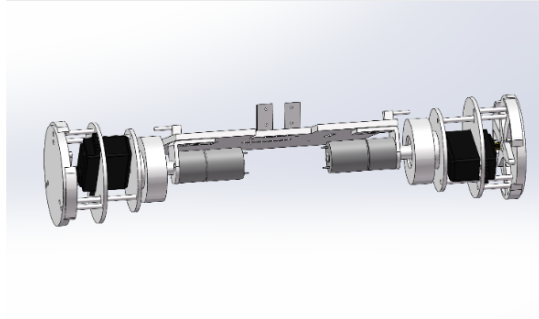


Fig. 2: CAD Drawing of the Two Wheel Design

B. Cam and Follower for Transformable Wheel

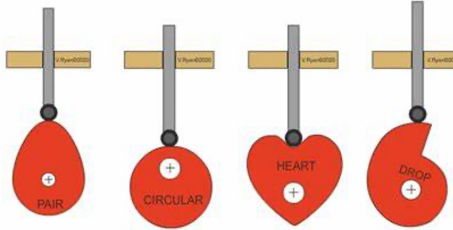


Fig. 3: Comparison of Different Cam and Follower Models

A comparison of the different cam model for the cam and follower mechanism was analysed. From the findings, a decision was made to stick with the traditional Pair cam and follower design. By using the traditional cam and follower Pair design, the feet of the transformable wheel can be extended at a high velocity, as shown in the velocity profile Fig. 4.

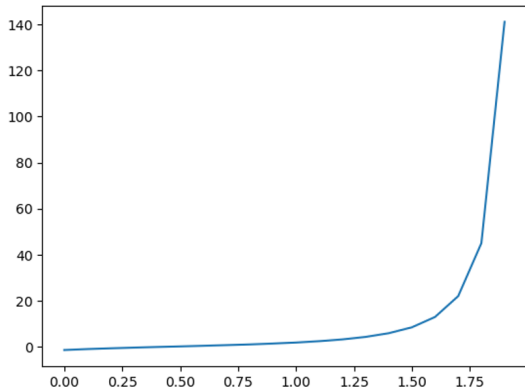


Fig. 4: Velocity Profile of the Follower (θ)

As the transformable wheel requires the center cam to extend the three separate feet at the same time, it was easier to design and manufacture the cam rotor normally into a triangular shape.

C. Graphical Linkage Synthesis

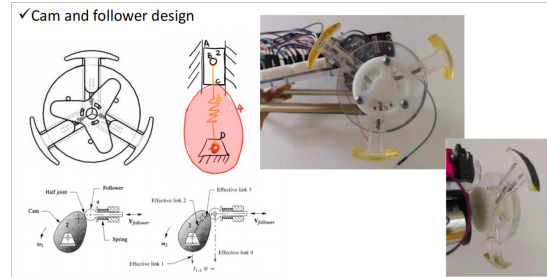


Fig. 5: Graphical Synthesis of the Wheel

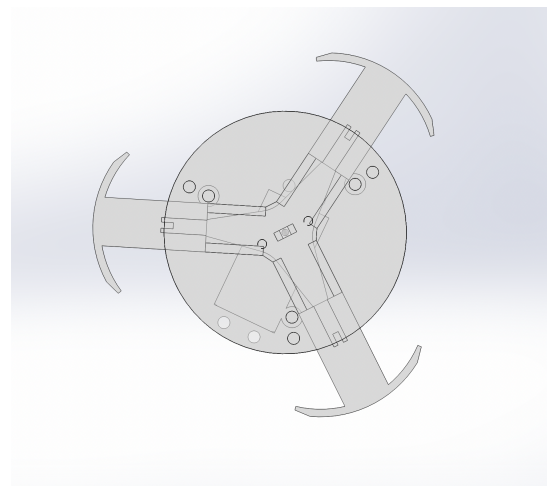


Fig. 6: Transformable Wheel in Fully Extended Position

The feet of the transformable wheel are fitted within a slot, this then is the slider for the cam and follower mechanism. As observe from the expanded and shrunk modes are shown in the Fig. 5 and Fig. 6. Each of the transformable wheel consists of 5 links, with 4 full joints, and 3 half joints. The cam and follower mechanism used in the vehicle are classified as half joints. Hence, the Degree of Freedom calculated is 1. An additional spring is attached to each feet with the wheel to allow the feet to retract back to it's original shrunken position.

III. MANUFACTURING - FABRICATION AND ASSEMBLY

A. Material Selection

The main structure of the vehicle should be able to withstand bending, but the weight of the material cannot be large as the car needs to be able to travel up steps, and not sink on sandy terrain. From the lecture, a quantity $\frac{K}{m}$, where K is the bending stiffness, m is the mass, can be used as a criterion for material selection. The higher this value is, the tougher it is.

$$K = \frac{3EI}{L^3}, \quad (1)$$

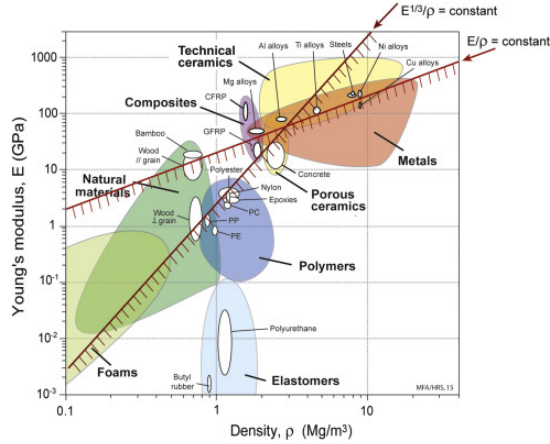


Fig. 7: Material selection criteria.

where E is the Young's Modulus, I is the moment of inertia, and L is the length of the part. And the part has a mass of

$$m = \rho L h b. \quad (2)$$

Therefore, $\frac{K}{m}$ has a linear relationship with material property $\frac{E}{\rho}$. Based on the Ashby and Cebon's graph 7, it shows that acrylic is an optimal choice for the vehicle, therefore the main base of our vehicle is constructed with acrylic.

The vehicle wheels and parts are constructed with 3D printed extrusion of Polylactic acid (PLA). PLA was selected as the material for the wheels as the parts needed to be 3D printed.

Spring: Stainless steel

The spring is made of stainless steel. Stainless steel has a very high yield strength and shear modulus. This allows objects made of stainless steel to return to their original shape despite significant deflection or twisting.

B. Fabrication Methods

1) Laser Cutting: The acrylic baseplate of the vehicle is fabricated through laser cutting. Laser cutting provides high precision and accuracy, essential for creating intricate and detailed parts from acrylic. In addition, laser cutting is relatively fast, enabling quick turnaround times for producing parts, and produces clean and smooth edges, reducing the need for post-processing.

2) 3D Printing: For the transformable wheels of the vehicle, the components are 3D printed. Since the components of the transformable wheels are unique, they had to be designed and manufactured in-house. Therefore, in this case, there is a need to utilize 3D printing to optimize the manufacturing efficiency of the parts.

C. Motor Selection



JGA25-370 Geared Motor

Fig. 8: Selected Motor

Voltage V	No-load		Maximum efficiency pointed				Blockage	
	speed r/min	electric current A	speed r/min	electric current A	Torque Kg.cm	Power W	Torque Kg.cm	electric current A
	6	190	0.2	133	0.5	0.75	1.1	4.0
12	350	0.1	245	0.65	1.4	2.4	5.2	2.2

Fig. 9: Selected Motor Specifications

Based on the calculation done in the Force analysis section, the motor selected is the JGA25-370 geared motor. It uses a gear set to convert the original high speed and low torque of the motor to a low speed and high torque. The selected motor specifications are shown in Fig. 9 above.

D. Assembly of Components

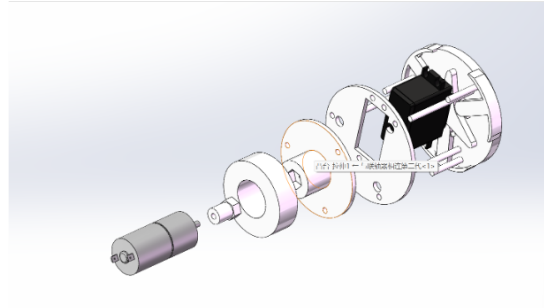


Fig. 10: Assembly of Transformable Wheel

1) Assembly of the Transformable Wheel: The feet of the transformable wheel need to be able to move within the slider for the cam and follower mechanism. The servo motors control the extension of the feet. A spring is attached to each of the three feet to allow the feet to be quickly retracted after crossing the obstacles. Thus, the servo motors are attached to the cam in order to drive the cam and follower mechanism to extend the feet of the transformable wheel. The DC motor is attached to a slip ring in each wheel to ensure the wires do not tangle when the vehicle is in motion. The model and assembly diagram is shown in Fig. 10.

2) *Assembly of Sensors*: Three ultrasonic sensors are attached to the vehicle. One is installed at the front of the car to detect the obstacles in front, before activating the transformable wheel, and the other two are at the right and left to ensure the vehicle does not collide with any barriers and for straight driving. A camera is used to register the green arrow that will determine the vehicle traveling direction.

IV. CONTROL OF SENSORS AND ACTUATORS

A. Flowchart

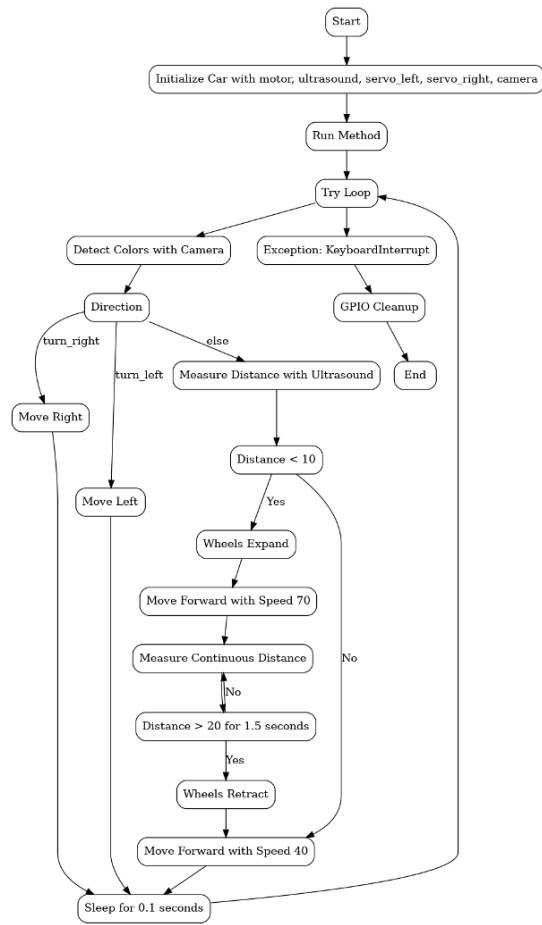


Fig. 11: General Flowchart

The process begins by initializing the car with a motor, ultrasound sensor, servos (left and right), and a camera. The main operation method is executed within a try loop to handle exceptions. The car first uses the camera to detect colors and determine the direction: it moves right if the detected color indicates a right turn or moves left otherwise. If no color-based direction is determined, the car measures the distance ahead using the ultrasound sensor. If the distance is less than 10 units, the car expands its wheels and moves forward at speed 70, continuously measuring the distance. If the distance exceeds 20 units for 1.5 seconds, the wheels retract, and the car slows down to speed 40. After each cycle, the car pauses for 0.1 seconds before repeating the loop. In case of a KeyboardInterrupt exception, the GPIO

pins are cleaned up, and the process ends. The logic for the movement and different actions is shown in Fig. 11. The code to implement the logic in the flowchart is shown in the Appendix. The logic for the movement and different actions is shown in Fig. 11. The code to implement the logic in the flowchart is shown in the Appendix.

B. Circuit Diagram

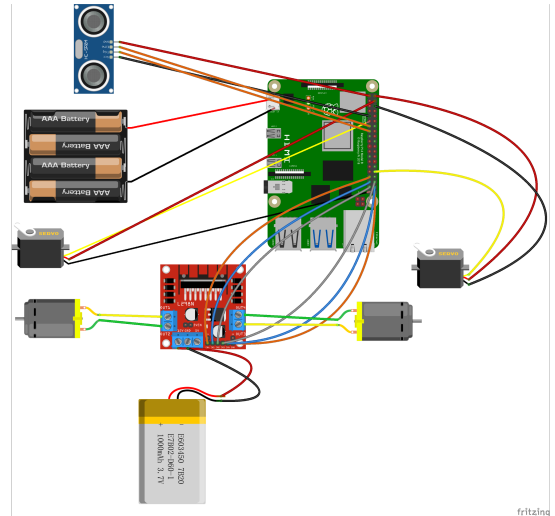


Fig. 12: Circuit Diagram

Fig. 12 depicts the circuit diagram of our project. A Raspberry Pi is used to connect and control all the other components. Three ultrasonic sensors are used for wall distance tracking and reorientation of the car. A camera is used to detect and recognize the arrow in the obstacle course. An L293D is used to drive the DC motors. The servo motors that control the mechanism in the transformable wheel are connected directly to the Raspberry Pi.

V. ANALYSIS

A. Classification of the Designed Linkage

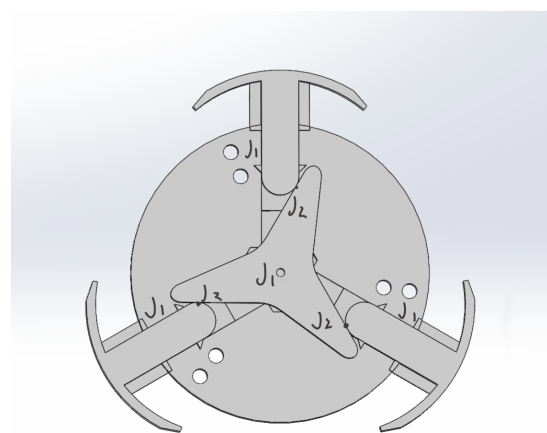


Fig. 13: Linkage Analysis of Wheel

C. Force and Torque Analysis

$$L = 5, J_1 = 4, J_2 = 3$$

$$DOF = 3(L - 1) - 2J_1 - J_2 = 1$$

The cam can fully rotate. The pivot of the three followers can be thought at the infinite. So they cannot fully rotate. Thus the transformable wheels are classified as a Type 2 Grashof Crank Rocker Rocker mechanism.

B. Position Analysis of the Cam and Follower

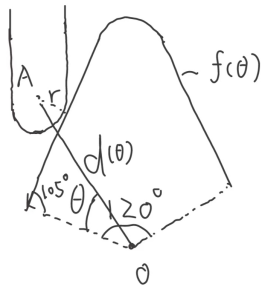


Fig. 14: Positional Analysis of the Cam and Follower

The polar coordinate function of the profile of the cam is

$$f(\theta) = \frac{10\sin(105)}{\sin(75 - \theta)}, \quad 0 \leq \theta < 55$$

$$f(\theta) = 28.242, \quad 55 \leq \theta < 65$$

$$f(\theta) = \frac{10\sin(105)}{\sin(\theta + 45)}, \quad 65 \leq \theta \leq 120$$

The distance AO is

$$d(\theta) = f(\theta) + \frac{r}{\sin(75 - \theta)}$$

Then we use MATLAB to plot it.

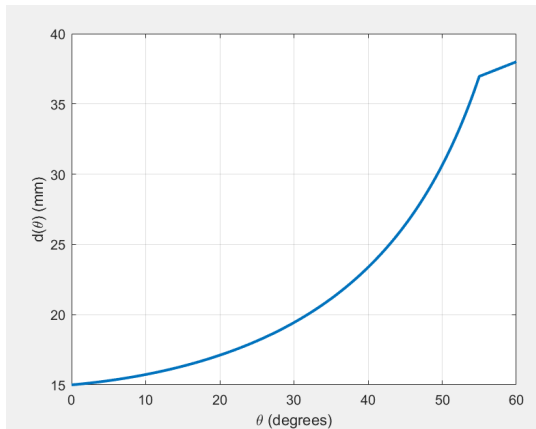


Fig. 15: Distance of AO Versus Rotation Angle

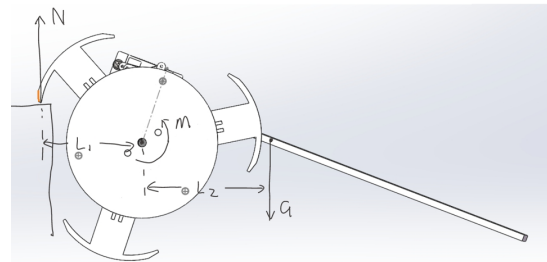


Fig. 16: Free Body Diagram When Climbing Up

1) Force Analysis of Motor:

$$\Sigma F_y = N - G = 0$$

$$\Sigma M = 2M - NL_1 - GL_2 = 0$$

$$M = \frac{NL_1 + GL_2}{2} = \frac{G}{2}(L_1 + L_2)$$

Where L_1 is a variable and L_2 is an invariant.

$$0 \leq L_1 \leq 5\text{cm}, \quad L_2 = 3\text{cm}, \quad G = 1\text{kg}$$

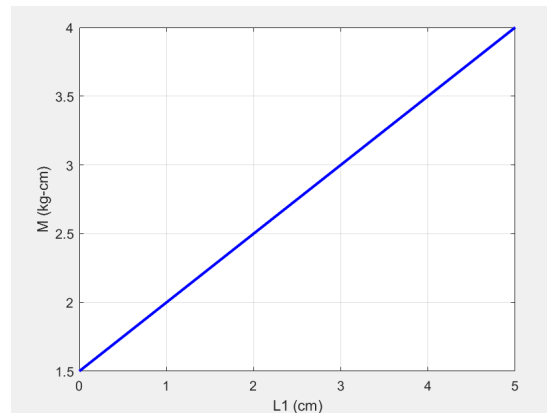


Fig. 17: Torque Needed Versus Distance

The motor requires a maximum torque of $4\text{kg} \cdot \text{cm}$ for the wheel to climb over obstacles. Our selected motor has a torque of $5.5\text{kg} \cdot \text{cm}$ when blocked.

2) Force Analysis of Servo:

For the whole car:

$$\Sigma F_y = N_1 + N_2 - \frac{G}{2} = 0$$

$$\Sigma M = N_2 \cdot \frac{L}{2} - N_1 \cdot \frac{L}{2} = 0$$

$$N_1 = N_2 = \frac{G}{4}$$

For one foot:

$$\theta_1 = 60^\circ$$

$$\Sigma F_x = N_1 \cos \theta_1 - F \cos \theta_2 = 0$$

$$F = \frac{N_1 \cos \theta_1}{\cos \theta_2}$$

$$F = \frac{N_1 \cos 60^\circ}{\cos \theta_2} = \frac{N_1}{2 \cos \theta_2}$$

$$L_1 = r \sin \theta_2$$

$$M = F \cdot L_1 = \frac{N_1}{2 \cos \theta_2} \cdot r \sin \theta_2 = \frac{N_1 r}{2} \tan \theta_2 = \frac{Gr}{8} \tan \theta_2$$

For $r = 4\text{cm}$, $0^\circ \leq \theta_2 \leq 80^\circ$, $G = 0.8\text{kg}$:

$$M \leq 0.4 \cdot \tan 85^\circ = 4.57\text{kg} \cdot \text{cm}$$

The required servo's torque is $4.57\text{kg} \cdot \text{cm}$ for extending the feet. Our servo has a torque of $11\text{kg} \cdot \text{cm}$ which is enough.

3) Safety Factor: For the two couplings connected to the wheel:

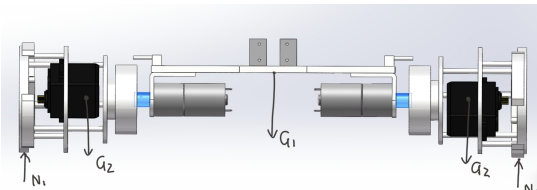


Fig. 18: Free Body Diagram of the Whole Car

$$N_1 = N_2 = \frac{G_1 + 2G_2}{2}$$

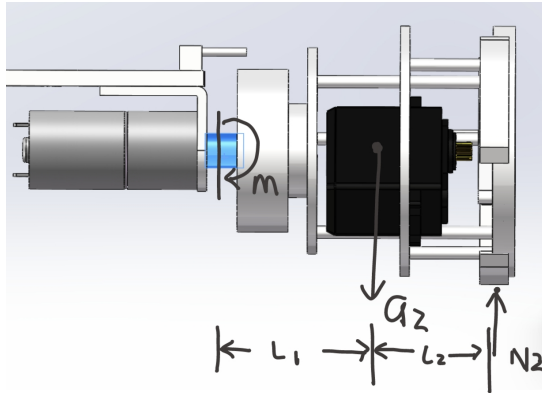


Fig. 19: Free Body Diagram of the Wheel

$$\Sigma M = -M - G_2 L_1 + N_2(L_1 + L_2) = 0$$

$$M = \frac{1}{2}[G_1(L_1 + L_2) + G_2(L_2 - L_1)] = 0.49N \cdot m$$

The secondary moment of inertia:

$$I = \frac{1}{4}\pi r^4 = 7.85 \times 10^{-9}m^4 \sigma = \frac{Mr}{I} = 0.624\text{Mpa}$$

The yield strength of copper is 33Mpa . The safety factor against yielding:

$$X = \frac{33\text{Mpa}}{0.624\text{Mpa}} = 53 >> 1$$

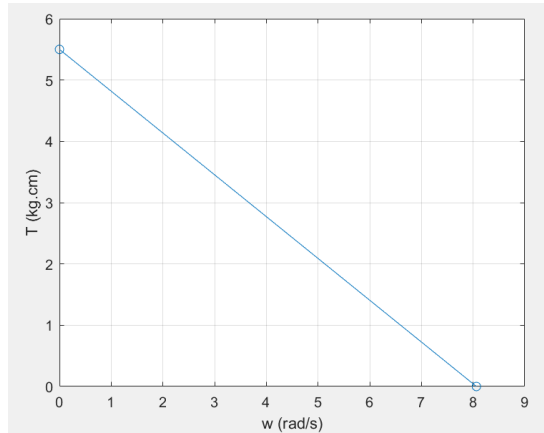


Fig. 20: Torque vs Angular Velocity

4) Rolling Speed Analysis: Our vehicle remains in a contracted state while rolling on both smooth surfaces and sandy terrain.

$$\omega = -1.47T + 8.12$$

On the smooth surface

$$\Sigma F_y = N_1 + N_2 + N_3 - G = 0$$

$$\Sigma M = (N_2 + N_3) \cdot \frac{L}{5} - N_1 \cdot \frac{4L}{5}$$

$$N_1 = \frac{G}{5}, \quad N_2 = N_3 = \frac{2G}{5}$$

$$N_1 = 0.2\text{kg}, \quad \mu = 0.3$$

$$\Sigma F_x = N_1 \mu - f = 0$$

$$T = fr = 0.24\text{kg} \cdot \text{cm}$$

$$\omega = -1.47 \cdot 0.24 + 8.12 = 7.77\text{rad/s}$$

If retracted

$$v = \omega \cdot r_1 = 0.312\text{m/s}$$

If expanded

$$v = \omega \cdot r_1 = 0.466\text{m/s}$$

On the sand

$$G = 1\text{kg}, \quad \mu = 1$$

$$\Sigma F_x = G\mu - f = 0$$

$$T = fr = 4\text{kg} \cdot \text{cm}$$

$$\omega = -1.47 \cdot 4 + 8.12 = 2.24\text{rad/s}$$

If retracted

$$v = \omega \cdot r_1 = 0.089\text{m/s}$$

If expanded

$$v = \omega \cdot r_2 = 0.134\text{m/s}$$

VI. EXPERIMENT

A. Load Carrying Capacity

To measure the maximum carrying capacity, we put weights on the car and tested whether it can climb onto the sandbox. A 500g load was added after each successful test. When the weights reached 2.5 kg, visible deformation of the base occurred, but the motors were still able to lift the car; when the weights reached 3.0 kg, the motor was overloaded and the wheels failed. See the attached video clip for the whole test.

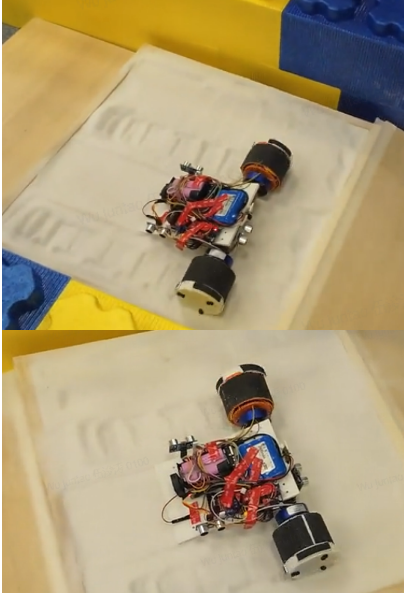


Fig. 21: The performance with 2.5kg load (left) and 3.0kg load (right).

Since the weight of the car itself is 1.4 kg, the total maximum load adds up to

$$M_{\max} = 1.4\text{kg} + 2.5\text{kg} = 3.9\text{kg}$$

With the same calculation method as stated in Analysis part, we obtain the maximum torque

$$T_{\max} = rF \sin(\theta) = 3.084\text{N} \cdot \text{m} = 31.47\text{kg} \cdot \text{cm}$$

This is a slight mismatch with our analysis, which states that the rated load of one motor is 15kg-cm. The error is

$$T_{\text{err}} = \frac{(31.47 - 30)}{2 \times 15} \times 100\% = 4.9\%$$

We think this error is acceptable. The error might have come from:

- 1) The supporting force of the ground, which wasn't taken into account in analysis.
- 2) The mismatch of the actual load with the rated load of our motors.

B. Climbing Performance

Our wheel can expand due to the rotation of the cam upon encountering the barriers. The mechanism is shown in other sections. And the real photo is listed here:

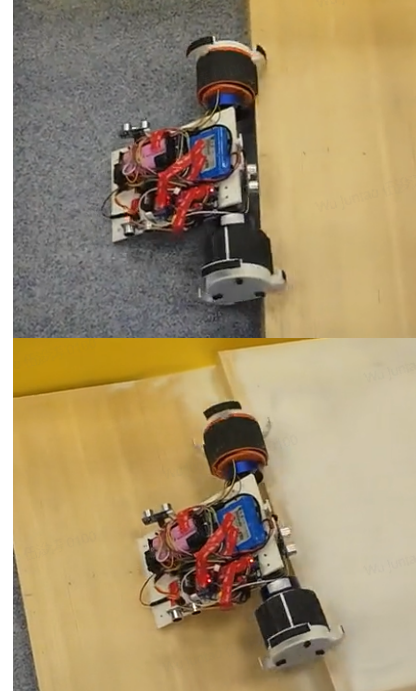


Fig. 22: The climbing performance

C. Rolling Performance

We used a 0.02mm-precision caliper to measure the diameter of the closed wheel, and a 1mm-precision ruler for the radius of the open wheel. The theoretical value is calculated from CAD dimensions. The results are as follows.

	Actual dimension [mm]	Theoretical value [mm]	Error
Expansion	180.0	178.5	0.84%
Shrinkage	89.20	88.50	0.79%

TABLE I: The dimensions of the wheel.

The precision of our wheel is high, since the error of laser cutting is usually less than $\pm 0.2\text{mm}$. Except for that, we think the error might come from:

- 1) The thickness of hot-melt glue on the outer surface of the wheel;
- 2) Measuring errors.

To measure the speed of the car, we conducted 5 tests and calculated the average value. The results are listed below. The results of the previous analysis are used to calculate the rotation speed. We compare the rotation speed with the rated speed of the motor, which is 30 RPM. Three significant digits are kept for all the calculations.

1) *Speed on Smooth Surface*: The error could come from the mismatch of the rated rotation speed and the actual speed of the motor, which is due to the load. A 15.3 percent mismatch is considered acceptable.

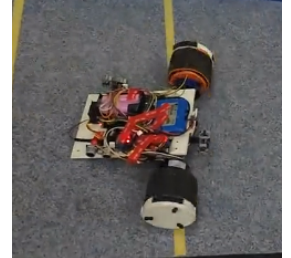
2) *Speed on Sand*: We observe a significant speed mismatch here. To eliminate the effect of the motor, we will calculate the deviation again, with the actual motor speed (26.1 rpm) obtained in the previous part:

	speed [m/s]	speed [rpm]	deviation from theoretical value
Trial 1	0.121	26.1	
Trial 2	0.121	26.1	
Trial 3	0.121	26.1	
Trial 4	0.105	22.6	abnormal data
Trial 5	0.121	26.1	
Average	0.118	25.4	15.3%

TABLE II: The speed on smooth surface.



((a))



((b))

Fig. 24: Experiments of going through a 10-cm-high tunnel.
(a) Model A. (b) Model B.

	speed [m/s]	speed [rpm]	deviation from theoretical value
Trial 1	0.103	13.1	
Trial 2	0.130	16.7	
Trial 3	0.125	16.1	
Trial 4	0.133	17.1	
Trial 5	0.138	17.8	
Average	0.126	16.2	20.0%

TABLE III: The speed on sand.

$$T_{\text{err}} = \frac{16.2 - 26.1}{26.1} \times 100\% = 37.9\%$$

The reason for the difference between the real value and the theoretical result is that we cannot calculate the resistance in the sand. Under the load in the sand, the rotation speed of the motor will decrease. The higher the resistance, the lower the speed will be. The speed given by the manufacturer is measured under no load. The reason that the speed in the sand is lower than the one on the smooth surface is because the wheel will experience more resistance in the sand. Also, the torsion spring helps close the trigger leg, thus reducing the radius of the wheel. The result we calculate matches our expectations.

D. Wheels Transformability Performance

The wheel robots are able to adapt to different kinds of surroundings. They can climb up a 6-cm-high step in stretching mode as shown in Fig. 25, and go through a 10-cm-high tunnel in shrinking mode as shown in Fig. 26.



((a))



((b))

Fig. 23: Experiments of climbing a 6-cm-high step. (a) Model A. (b) Model B.

VII. DISCUSSION

Based on detailed analysis and results from trial and errors that have been done in the development of this autonomous

¹See the attached video clip for demonstration.

transformable wheel vehicle, we can agree with other current researches on the success rate of the climbing performances of the vehicle. However, compared to other current researches, there are 2 factors that puts our autonomous transformable wheel vehicle ahead. The factors mentioned previously is as of follows:

- The time taken for our wheel to expand is 0-3 seconds while other researches on average takes about 0-5 seconds making our autonomous transformable wheel vehicle more efficient.
- Our prototype autonomous transformable wheel vehicle is moderately low-cost and lightweight model product compared to other current research that have been developed.

Although our autonomous transformable wheel vehicle has some competitive advantages against current researches, there also some disadvantages our model. These disadvantages is as of follows:

- The load carrying capacity of our autonomous transformable wheel vehicle is comparatively bad to other current research.
- The speed our autonomous transformable wheel vehicle is slow on certain surfaces such as sand while other researches are able to maintain similar speeds in different surfaces.

Knowing this, our development team plans to address these issues by increasing the servo torque, motor speed, and tire friction coefficient. As a result, after successfully addressing these issues and by scaling our autonomous transformable wheel vehicle to the demands of the market, the applications of our model are limitless as it can go and explore certain terrains that are too dangerous for us to explore ourselves; ranging from discovery to military applications.

VIII. CONCLUSION

This paper proposes a transformable wheel autonomous vehicle and draws the conclusions as follows.

- 1) This autonomous transformable wheel vehicle can navigate through various test terrains, pass through height restrictions, traverse sand, and climb stairs.
- 2) This autonomous transformable wheel vehicle can adjust its posture and direction based on the terrain using

the applied ultrasonic sensors on its front, right, and left rear guard.

- 3) Our innovative cam-follower-spring wheel can easily expand and contract on any terrain while the transformable wheel can easily lift the car.
- 4) The load-bearing capacity of the cam-follower-spring wheel is not as effective yet compared to other current research as carrying too heavy an object prevents the wheels from expanding.
- 5) This paper analyzes the motions of the autonomous transformable wheel vehicle in wheeled and expanded mode as it goes through the set terrain with different height and surfaces.
- 6) The speed of this autonomous transformable wheel vehicle is slow on sand compared to other current research. These issues can be solved by increasing the servo torque, motor speed, and tire friction coefficient, which we plan to validate in future improvements.
- 7) One competitive advantage our autonomous transformable wheel vehicle has compared to other current research is that it provides the industry with a low-cost and lightweight model product.
- 8) The transformable wheels play a critical role in enhancing the performance of a vehicle due to their superior traction, stability, and shock absorption compared to rigid wheels which allow it to maneuver through different terrains. If scaled and developed correctly, its applications in the real-world are limitless.

APPENDIX

A. Literature Review

No.	Product Name	Capabilities	Problems	Ref.
L1	Mobility Analysis of a Spoked Walking Machine With Variable Topologies	Has incredible and maneuverability versatility due to its unique design and use of material	- none yet -	[[1], Ren, P.]
L2	Bio-inspired design and dynamic maneuverability of a minimally actuated six-legged robot	Demonstrates turning and rapid running in a small underactuated legged robot.	Inconsistency may arise due to differences in gait kinematics and scale between our robot and the cockroaches studied	[[2], A. M. Hoover]
L3	The Deformable Wheel Robot Using Magic-ball Origami Structure	Easy to make fold line and also has high shear resistance	total displacement of passive decreases due to the stiffness of the structure, friction of the shaft and not enough force of the SMA spring, the deformed diameter of the wheel is much bigger than the theoretical value.	[[3], Lee, D]
L4	Buckling of Elastomeric Beams Enables Actuation of Soft Machines	Incredible performances in shrinking on actuation and torsional motion while also maintaining durability.	the maximum force they can generate is limited by the pressure differential over which they operate.	[[4], Yang, D.]

L5	Development of a Transformable Wheel Actuated by Soft Pneumatic Actuators	the wheel can be transformed under a heavy payload with little air pressure	high payload has potential to cause the large impact force and high collision speed, which may result in damage to the wheel structure, the robot body and the transmission	[[5], Yun, SS.]		The behavioral performance of the robot in both wheeled and legged modes is experimentally evaluated. As expected, the robot in wheeled mode yields a smoother ride and better power efficiency. On the other hand, the robot in legged mode has better mobility to cross obstacles or rough terrains.	
L6	A Transformable Wheel Robot with A Passive Leg	demonstrates that the robot is able to transform under a heavy payload with the passive leg actuation	-none yet-	[[6], Yu She]	Quattroped: A Leg-Wheel Transformable Robot		-none yet- [[9], S. -C. Chen]
L7	Wheel Transformer: A Wheel-Leg Hybrid Robot With Passive Transformable Wheels	stable and energy-efficient driving ability of circular wheels with incredible obstacle climbing ability of legged wheels.	weak agility and motor capabilities	[[7], Y. -S. Kim]	A transformable wheel-legged mobile robot: Design, analysis and experiment	incredible success rate at climbing obstacles at different heights	-none yet- [[10], Tao Sun]
L8	Deformable Wheel Robot based on Soft Material	a high degree of adaptability to the environment.	a large number of actuators can present problems in manufacturing and control and the transmission structure is prone to breakage when high torque is applied to the wheel	[[8], Lee, DY.]			

B. Gantt Chart



C. Code

```

import time
import numpy as np
import RPi.GPIO as GPIO
from gpiozero_extended import Motor, PID
#try this code on the car
GPIO.setmode(GPIO.BCM)
class EchoSensor:
    def init(self, trigPin = 15, echoPin =
13):

```

```

self.trigPin = trigPin
self.echoPin = echoPin
t0 = time.perf_counter()
while(t1 < t0 + 3):
    t1 = time.perf_counter()
    if self.get_dist() < 3:
        self.hand = True
        break
    else:
        self.hand = False
def get_dist(self):
    while True:
        # setup the trigger pin
        GPIO.output(self.trigPin,0)
        time.sleep(2E-6)
        GPIO.output(self.trigPin,1)
        time.sleep(10E-6)
        GPIO.output(self.trigPin,0)
        # measure with the echo pin
        while GPIO.input(self.echoPin)==0:
            pass
        echoStartTime = time.time()
        while GPIO.input(self.echoPin)==1:
            pass
        echoStopTime = time.time()
        pingTravelTime = echoStopTime -
            echoStartTime
        # speed of sound is 343 m/s, 34300
        # cm/s at 20 degree celcius
        echoTravelDistance =
            pingTravelTime*34300
        print(round(self.distance,1),' cm')
        time.sleep(0.2)
        return echoTravelDistance/2
#put the configuration pins in here
echoL = EchoSensor(trigPin =7, echoPin = 8)
echoR = EchoSensor(trigPin =6, echoPin = 5 )
maxDist_diff = 40
def turnLeft():
    tstart = time.time()
    tstop = tstart
    while tstop < tstart + 3:
        tstop = time.time()
        mymotorL.set_output(0)
        mymotorR.set_output(1)

def turnRight():
    tstart = time.time()
    tstop = tstart
    while tstop < tstart + 3:
        tstop = time.time()
        mymotorL.set_output(1)
        mymotorR.set_output(0)

# Setting general parameters
tstop = 2 # Execution duration (s)
tsample = 0.01 # Sampling period (s)
wsp = 1 # Motor speed set point (rad/s)
wmax = 100 # Maximum motor speed (rad/s) for
    scaling
tau = 0.1 # Speed low-pass filter response
    time (s)
distance = 0
ena = 16
in1 = 20
in2 = 21
enb = 13
in3 = 26
in4 = 19
# Creating PID controller object
kp = 0.15
ki = 0.35
kd = 0.01
taupid = 0.01
pid = PID(tsample, kp, ki, kd, umin=0,
    umax=1, tau=taupid) # Ensuring umax is
    set to 1

# Creating motor object using GPIO pins 16,
    17, and 18
#without encoder
mymotorL = Motor(enable1=enb, pwml=in3,
    pwm2=in4 )
mymotorR = Motor(enable1=ena, pwml=in1,
    pwm2=in2 )
#mymotor.reset_angle()

# Initializing previous and current values
ucurr = 0 # x[n] (step input)
Dist_diff_prev = 0 # y[n-1]
Dist_diff_curr = 0 # y[n]

# Initializing variables and starting clock
thetaprev = 0
tprev = 0
tc curr = 0
tstart = time.perf_counter()

# Running execution loop
print('Running code for', tstop, 'seconds
    ...')
try:
    while True:
        #get distance of the sensor
        # Pausing for 'tsample' to give CPU
            time to process encoder signal
        distL = echoL.get_dist()
        distR = echoR.get_dist()
        if(distL > 30 and distR > 30):
            if(echoL.hand and echoR.hand):
                turnLeft()
            else:
                turnRight()
        time.sleep(tsample)
        # Getting current time (s)
        tc curr = time.perf_counter() - tstart
        # Getting motor shaft angular
            position: I/O (data in)
        #thetacurr = mymotor.get_angle()
        # Calculating motor speed (rad/s)
        #wcurr = np.pi / 180 * (thetacurr -
            thetaprev) / (tc curr - tprev)
        # Filtering motor speed signal
        #wfc curr = tau / (tau + tsample) *
            wfprev + tsample / (tau + tsample)
            * wcurr
        Dist_diff_curr = distL - distR
        Dist_diff_prev = Dist_diff_curr
        # Scaling speed measurement to [0, 1]
        #wfc curr_scaled = wfc curr / wmax
        #wsp_scaled = wsp / wmax
        # Calculating closed-loop output
        ucurr = pid.control(0, Dist_diff_curr)
        ucurr_scaled = ucurr / maxDist_diff
        # Assigning motor output: I/O (data
            out)

```

```

mymotorL.set_output(ucurr_scaled + wsp)
mymotorR.set_output(-ucurr_scaled +
    wsp)
# Updating previous values



---



```

REFERENCES

- [1] Ren, P., and Hong, D. (September 26, 2011). "Mobility Analysis of a Spoked Walking Machine With Variable Topologies." ASME. J. Mechanisms Robotics. November 2011; 3(4): 041005. <https://doi.org/10.1115/1.4004892>
- [2] A. M. Hoover, S. Burden, Xiao-Yu Fu, S. Shankar Sastry and R. S. Fearing, "Bio-inspired design and dynamic maneuverability of a minimally actuated six-legged robot," 2010 3rd IEEE RAS and EMBS International Conference on Biomedical Robotics and Biomechatronics, Tokyo, Japan, 2010, pp. 869-876, <https://doi:10.1109/BIOROB.2010.5626034>.
- [3] Lee, D., Kim, J., Kim, S., Koh, J., and Cho, K. "The Deformable Wheel Robot Using Magic-Ball Origami Structure." Proceedings of the ASME 2013 International Design Engineering Technical Conferences and Computers and Information in Engineering Conference. Volume 6B: 37th Mechanisms and Robotics Conference. Portland, Oregon, USA. August 4–7, 2013. V06BT07A040. ASME. <https://doi.org/10.1115/DETC2013-13016>
- [4] Yang, D., Mosadegh, B., Ainla, A., Lee, B., Khashai, F., Suo, Z., Bertoldi, K. and Whitesides, G.M. (2015), Buckling of Elastomeric Beams Enables Actuation of Soft Machines. *Adv. Mater.*, 27: 6323-6327. <https://doi.org/10.1002/adma.201503188>
- [5] Yun, SS., Lee, JY., Jung, GP. et al. Development of a transformable wheel actuated by soft pneumatic actuators. *Int. J. Control Autom. Syst.* 15, 36–44 (2017). <https://doi.org/10.1007/s12555-016-0477-9>
- [6] Yu She, C. J. Hurd and H. -J. Su, "A transformable wheel robot with a passive leg," 2015 IEEE/RSJ International Conference on Intelligent Robots and Systems (IROS), Hamburg, Germany, 2015, pp. 4165-4170, doi: 10.1109/IROS.2015.7353966.
- [7] Y. -S. Kim, G. -P. Jung, H. Kim, K. -J. Cho and C. -N. Chu, "Wheel Transformer: A Wheel-Leg Hybrid Robot With Passive Transformable Wheels," in *IEEE Transactions on Robotics*, vol. 30, no. 6, pp. 1487-1498, Dec. 2014, doi: 10.1109/TRO.2014.2365651.
- [8] Lee, DY., Koh, JS., Kim, JS. et al. Deformable-wheel robot based on soft material. *Int. J. Precis. Eng. Manuf.* 14, 1439–1445 (2013). <https://doi.org/10.1007/s12541-013-0194-8>
- [9] S. -C. Chen, K. -J. Huang, W. -H. Chen, S. -Y. Shen, C. -H. Li and P. -C. Lin, "Quattroped: A Leg-Wheel Transformable Robot," in *IEEE/ASME Transactions on Mechatronics*, vol. 19, no. 2, pp. 730-742, April 2014, doi: 10.1109/TMECH.2013.2253615.
- [10] Tao Sun, Xu Xiang, Weihua Su, Hang Wu, Yimin Song, A transformable wheel-legged mobile robot: Design, analysis and experiment, *Robotics and Autonomous Systems*, Volume 98, 2017, Pages 30-41, ISSN 0921-8890, <https://doi.org/10.1016/j.robot.2017.09.008>.



FIRST A.AUTHOR Li Siyuan is a sophomore mechanic engineering and computer science dual degree student in UM-SJTU Joint Institute. He is responsible for the manufacturing of the whole car, electronic control and part of the algorithm.



SECOND B.AUTHOR Juntao Wu is a sophomore mechanic engineering and computer engineering dual degree student in UM-SJTU Joint Institute. He is responsible for electronic control and the algorithm.



THIRD C.AUTHOR Sergio Aman Soetomo is a junior Mechanical Engineering Undergraduate Degree student in the UM - SJTU Joint Institute. He contributed for the report writing, prototype testing and assembly.



FOURTH D.AUTHOR Koh Hock Jin is a senior Mechanical Engineering Undergraduate Degree student in the UM - SJTU Joint Institute. He contributed for the report writing and prototype testing.